A new convergent and universally bounded interpolation scheme for the treatment of advection: application to viscoelastic simulations

M.A. Alves[1], P.J. Oliveira[2], F.T. Pinho[3]

[1] *Departamento de Engenharia Química, CEFT, Faculdade de Engenharia da Universidade do Porto (Portugal).*
[2] *Departamento de Engenharia Electromecânica, Universidade da Beira Interior (Portugal).*
[3] *Centro de Estudos de Fenómenos de Transporte, DEMEGI, Faculdade de Engenharia da Universidade do Porto (Portugal).*

Introduction

Accurate predictions of viscoelastic flows require discretisation schemes for convection of at least second-order accuracy. In an important paper, Godunov [1] demonstrated that all monotone (bounded) linear schemes could be at most first-order accurate. The only way to avoid this limitation is thus the development of nonlinear composite schemes, usually referred to as high-resolution schemes (HRS). Several discretisation schemes were proposed in the last years based on either the total variation diminishing framework (TVD) [2], on the normalised variable formulation (NVF) [3], or others. The NVF approach has been extended to non-uniform grids yielding the normalised variable and space formulation (NVSF) [4], to be used here. Although HRS's have seen widespread usage in the last years, there are still some convergence difficulties with these methods [5]. This work aims at developing a new HRS with good accuracy and enhanced convergence properties. The new scheme, named Convergent and Universally Bounded Interpolation Scheme for the Treatment of Advection (CUBISTA), has similar accuracy to the well-known SMART scheme [6], both being third-order accurate on uniform meshes.

The upper-convected Maxwell (UCM) model was selected to assess the performance of the CUBISTA scheme due to the hyperbolic nature and the known numerical difficulties of these stress equations. The benchmark flow of a UCM fluid in a 4:1 planar contraction is used to compare the performance of different high-resolution schemes, and thus serving to illustrate the superiority of the CUBISTA scheme in terms of iterative convergence (robustness).

Governing Equations

The equations to be solved are those for mass and linear momentum conservation, and the constitutive equation for an UCM fluid, written in compact form as:

$$\frac{\partial u_i}{\partial x_i} = 0 \tag{1}$$

$$\rho \frac{\partial u_i}{\partial t} + \rho \frac{\partial u_j u_i}{\partial x_j} = -\frac{\partial p}{\partial x_i} + \frac{\partial \tau_{ij}}{\partial x_j} \tag{2}$$

$$\tau_{ij} + \lambda \left(\frac{\partial \tau_{ij}}{\partial t} + \frac{\partial u_k \tau_{ij}}{\partial x_k} \right) = \eta \left(\frac{\partial u_i}{\partial x_j} + \frac{\partial u_j}{\partial x_i} \right) + \\ \lambda \left(\tau_{jk} \frac{\partial u_i}{\partial x_k} + \tau_{ik} \frac{\partial u_j}{\partial x_k} \right) \tag{3}$$

where ρ, η and λ are the density, viscosity and relaxation time of the fluid, u_i and τ_{ij} are the Cartesian components of the velocity and extra stress tensor, and p is the pressure.

Numerical Method

The finite-volume numerical method used in this work to discretise Eqs. (1)-(3) is only briefly outlined below since it has already been described in detail [7,8]. A collocated mesh arrangement is used, in which all variables are calculated at the control-volume (cell) centres. The focus of this work is on the discretisation of the constitutive equation, which can be cast in the usual FV form as

$$a_{\mathrm{P}}\tau_{ij,\mathrm{P}} = \sum_{\mathrm{F}}^{6} a_{\mathrm{F}}\tau_{ij,\mathrm{F}} + S_{\tau_{ij}} \qquad (4)$$

where $\tau_{ij,\mathrm{P}}$ and $\tau_{ij,\mathrm{F}}$ represent the *ij*-component of the extra stress tensor at cell P and its neighbouring cells F, a_{P} and a_{F} are coefficients composed by convective fluxes, and $S_{\tau_{ij}}$ is the source term. The spatial discretisation of the governing equations is performed with central differences (CDS) and linear interpolation. The exceptions are the advective terms, which are discretised with the HRS implemented using the deferred correction approach [9] thus promoting stability, simplicity and memory savings [8].

High Resolution Schemes

We follow the Normalised Variable and Space Formulation (NVSF) of Darwish and Moukalled [4] which is an extension to non-uniform grids of the normalised variable formulation of Leonard [3]. In the NVSF approach, the advected stress component at cell face f is interpolated as

$$\tau_{ij,\mathrm{f}} = \tau_{ij,\mathrm{U}} + \widehat{\tau}_{ij,\mathrm{f}}\left(\tau_{ij,\mathrm{D}} - \tau_{ij,\mathrm{U}}\right) \qquad (5)$$

where the normalised face stress, $\widehat{\tau}_{ij,\mathrm{f}}$, is calculated using an appropriate nonlinear limiter. The subscripts U and D refer to the upstream and downstream cells to cell P, which is itself upstream to face f. The following limiters were selected for this work [4]:

(*i*) MINMOD

$$\widehat{\tau}_{ij,\mathrm{f}} = \max\left[\widehat{\tau}_{ij,\mathrm{P}}, \min\left(\frac{\widehat{\xi}_{\mathrm{f}}}{\widehat{\xi}_{\mathrm{P}}}\widehat{\tau}_{ij,\mathrm{P}}, \frac{1-\widehat{\xi}_{\mathrm{f}}}{1-\widehat{\xi}_{\mathrm{P}}}\widehat{\tau}_{ij,\mathrm{P}} + \frac{\widehat{\xi}_{\mathrm{f}}-\widehat{\xi}_{\mathrm{P}}}{1-\widehat{\xi}_{\mathrm{P}}}\right)\right] \quad (6)$$

(*ii*) SMART

$$\widehat{\tau}_{ij,\mathrm{f}} = \max\left[\widehat{\tau}_{ij,\mathrm{P}}, \min\left(\frac{\widehat{\xi}_{\mathrm{f}}(1-3\widehat{\xi}_{\mathrm{P}}+2\widehat{\xi}_{\mathrm{f}})}{\widehat{\xi}_{\mathrm{P}}(1-\widehat{\xi}_{\mathrm{P}})}\widehat{\tau}_{ij,\mathrm{P}},\right.\right.$$
$$\left.\left.\frac{\widehat{\xi}_{\mathrm{f}}(1-\widehat{\xi}_{\mathrm{f}})}{\widehat{\xi}_{\mathrm{P}}(1-\widehat{\xi}_{\mathrm{P}})}\widehat{\tau}_{ij,\mathrm{P}} + \frac{\widehat{\xi}_{\mathrm{f}}(\widehat{\xi}_{\mathrm{f}}-\widehat{\xi}_{\mathrm{P}})}{1-\widehat{\xi}_{\mathrm{P}}}, 1\right)\right] \quad (7)$$

(*iii*) CLAM

$$\widehat{\tau}_{ij,\mathrm{f}} = \max\left(\widehat{\tau}_{ij,\mathrm{P}}, \frac{\widehat{\xi}_{\mathrm{f}}-\widehat{\xi}_{\mathrm{P}}^{2}}{\widehat{\xi}_{\mathrm{P}}(1-\widehat{\xi}_{\mathrm{P}})}\widehat{\tau}_{ij,\mathrm{P}} - \frac{\widehat{\xi}_{\mathrm{f}}-\widehat{\xi}_{\mathrm{P}}}{\widehat{\xi}_{\mathrm{P}}(1-\widehat{\xi}_{\mathrm{P}})}\widehat{\tau}_{ij,\mathrm{P}}^{2}\right) \quad (8)$$

where the normalised variables $\widehat{\tau}_{ij,\mathrm{P}}$, $\widehat{\xi}_{\mathrm{P}}$ and $\widehat{\xi}_{\mathrm{f}}$ are defined as [4,8]:

$$\widehat{\tau}_{ij,\mathrm{P}} = \frac{\tau_{ij,\mathrm{P}} - \tau_{ij,\mathrm{U}}}{\tau_{ij,\mathrm{D}} - \tau_{ij,\mathrm{U}}} \qquad (9)$$

$$\widehat{\xi}_{\mathrm{P}} = \frac{\xi_{\mathrm{P}} - \xi_{\mathrm{U}}}{\xi_{\mathrm{D}} - \xi_{\mathrm{U}}}; \quad \widehat{\xi}_{\mathrm{f}} = \frac{\xi_{\mathrm{f}} - \xi_{\mathrm{U}}}{\xi_{\mathrm{D}} - \xi_{\mathrm{U}}} \qquad (10)$$

The CUBISTA high resolution scheme

The proposed scheme is a modified version of the SMART HRS satisfying TVD requirements in a proper way, leading to enhanced iterative convergence, as will be demonstrated below. The CUBISTA limiter is expressed in the NVSF as

$$\widehat{\tau}_{ij,\mathrm{f}} = \max\left\{\widehat{\tau}_{ij,\mathrm{P}}, \min\left[\left(1+\frac{\widehat{\xi}_{\mathrm{f}}-\widehat{\xi}_{\mathrm{P}}}{3(1-\widehat{\xi}_{\mathrm{P}})}\right)\frac{\widehat{\xi}_{\mathrm{f}}}{\widehat{\xi}_{\mathrm{P}}}\widehat{\tau}_{ij,\mathrm{P}},\right.\right.$$
$$\frac{\widehat{\xi}_{\mathrm{f}}(1-\widehat{\xi}_{\mathrm{f}})}{\widehat{\xi}_{\mathrm{P}}(1-\widehat{\xi}_{\mathrm{P}})}\widehat{\tau}_{ij,\mathrm{P}} + \frac{\widehat{\xi}_{\mathrm{f}}(\widehat{\xi}_{\mathrm{f}}-\widehat{\xi}_{\mathrm{P}})}{1-\widehat{\xi}_{\mathrm{P}}}, \qquad (11)$$
$$\left.\left.1-\frac{1-\widehat{\xi}_{\mathrm{f}}}{2(1-\widehat{\xi}_{\mathrm{P}})}\left(1-\widehat{\tau}_{ij,\mathrm{P}}\right)\right]\right\}$$

Note that $\widehat{\xi}_{\mathrm{P}}$ and $\widehat{\xi}_{\mathrm{f}}$ are geometric quantities, which are calculated once for each cell in the computational grid. Although the limiter functions look complex, its implementation in a general finite volume code is rather simple, if the deferred correction approach is used.

Results and Discussion

The popular 4:1 planar contraction flow of an UCM fluid is used to assess the accuracy and robustness of the proposed scheme, and to compare its performance with other commonly used HRS. The geometry and some of the relevant dimensions are sketched in Figure 1.
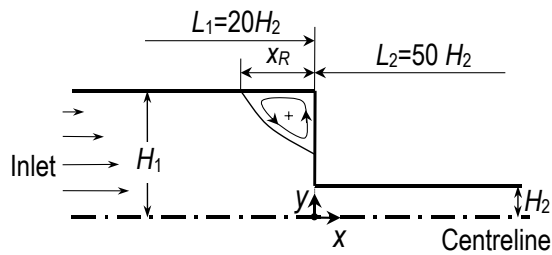

Figure 1. Geometry of the 4:1 planar contraction.

The flow domain was mapped with orthogonal but non-uniform meshes with increasing concentration of cells near the re-entrant corner and along the

downstream channel wall, where the stress gradients are expected to be higher. Calculations were carried out with two meshes, one with 3 598 cells (M1) and the other with 14 258 cells (M2). The cells adjacent to the re-entrant corner are squares with a non-dimensional size of 0.02 and 0.01 for meshes M1 and M2, respectively.

This flow is characterised by two dimensionless parameters, namely the Reynolds and Deborah numbers, here defined as $Re = \rho U_2 H_2 / \eta$ and $De = \lambda U_2 / H_2$. In the present calculations we take $Re = 0.01$, representative of creeping flow, and $De = 3$, which represents a moderate to high viscoelastic flow.

We have studied this problem in detail using very refined meshes (up to 57 032 cells) in conjunction with the MINMOD scheme [8]. Accurate solutions were obtained up to $De = 3$, which were recently validated independently by Aboubacar and Webster [10] using a cell-vertex finite volume/ element method. In the present work the goal is to study the convergence and accuracy properties of the proposed CUBISTA scheme, and to compare it with other HRS. The iterative convergence of the various HRS is illustrated in Figure 2, where the τ_{xx} residuals on mesh M1 are plotted as a function of the dimensionless elapsed time, $T=(U_2/H_2)\,t$. A steady-state converged solution is attained when the residuals of all variables fall below a tolerance of 10^{-4}.
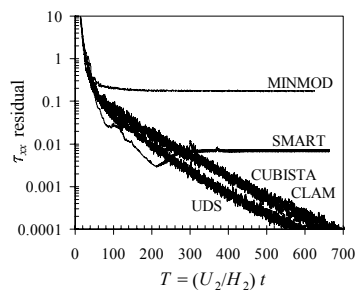
vanishing residuals. In the fine mesh M2, however, we found that only the UDS and CUBISTA schemes are able to attain iterative convergence, as illustrated in Figure 3. This figure proves the enhanced convergence properties of the proposed CUBISTA scheme, as compared to the other HRS.
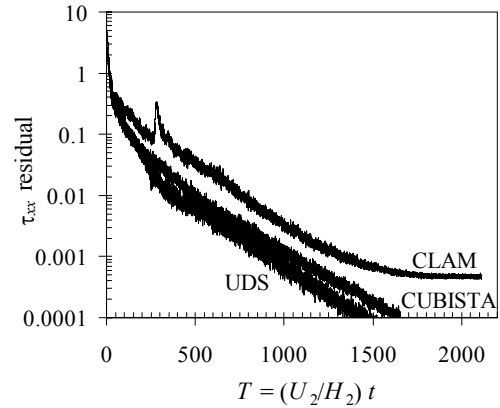

Figure 3. Decay of the L₁-norm of the τ_{xx} residuals (De=3; mesh M2).

To illustrate the accuracy of the CUBISTA scheme, Figure 4 shows a contour plot of the dimensionless first-normal stress difference. The more accurate (SMART) and less accurate (UDS) schemes are also shown for comparison purposes. The differences between the SMART and CUBISTA schemes are imperceptive, thus proving the good accuracy of the CUBISTA scheme.
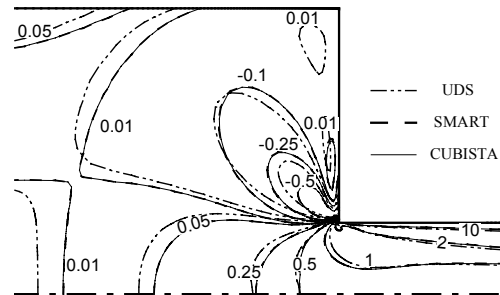

Figure 2. Decay of the L₁-norm of the τ_{xx} residuals for the various schemes at De=3 on mesh M1.

Figure 4. Contours of (τ_{xx}- τ_{yy})/($3\eta U_2/H_2$) obtained with the UDS, SMART and CUBISTA schemes on mesh M1.

Inspection of Figure 2 shows that both the MINMOD and the SMART schemes exhibit convergence difficulties. For this mesh, the CLAM and CUBISTA schemes show similar convergence rates, while the first-order UDS is a little faster to attain full convergence in terms of

As a final demonstration of the good accuracy of the CUBISTA scheme, in Figure 5 the streamline patterns obtained in the coarse mesh M1 with the UDS and CUBISTA schemes are compared to a highly accurate solution (calculated in a mesh with 57 032 cells, and presented in [8]).
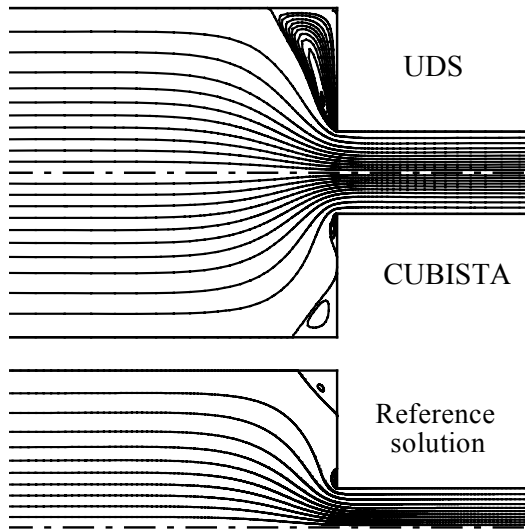
Figure 5. Streamline patterns obtained on mesh M1 for the UDS, SMART and CUBISTA schemes. Comparison with a highly accurate solution presented in [8].

As observed in Figure 5, the results obtained with the CUBISTA schemes are in close agreement with the mesh-independent solution. On the other hand, the UDS results exhibit an artificially enhanced corner vortex, a consequence of its low-order accuracy.

Acknowledgements

References

1. Godunov, S. K. (1959). Mat. Sbornik 47, 357-393.

2. Sweby, P.K. (1984). SIAM J. Numer. Anal. 21, 995-1011.

3. Leonard, B.P. (1988). Int. J. Numer. Meth. Fluids 8, 1291-1318.

4. Darwish, M.S., and Moukalled, F. (1994). Numer. Heat Transfer Part B 26, 79-96.

5. Zhu, J. (1992). Comput. Methods Appl. Mech. Engrg. 98, 345-360.

6. Gaskell, P.H., and Lau, A.K.C. (1988). Int. J. Numer. Meth. Fluids 8, 617-641.

7. Oliveira, P.J., Pinho, F.T., and Pinto, G.A. (1998). J. Non-Newt. Fluid Mech. 79, 1-43.

8. Alves, M.A., Pinho, F.T., and Oliveira, P.J. (2000). J. Non-Newt. Fluid Mech. 93, 287-314.

9. Khosla, P.K., and Rubin, S.G. (1974). Computers and Fluids 2, 207-209.

10. Aboubacar, M., and Webster, M.F. (2001). J. Non-Newt. Fluid Mech. 98, 83-106.

Contact Address:

P.J. Oliveira (pjpo@ubi.pt)
Dpto. Engenharia Electromecânica, Universidade da Beira Interior, 6201-001 Covilhã, Portugal.
Telf.: +351 275329952; Fax:+351 275329972.